# The contribution of TASK-1-containing channels to the function of dorsal lateral geniculate thalamocortical relay neurons

Sven G. Meuth, M. Isabel Aller, Thomas Munsch, Thekla Schuhmacher, Thomas Seidenbecher, Patrick Meuth, Christoph Kleinschnitz, Hans-Christian Pape, Heinz Wiendl, William Wisden and Thomas Budde

Institut für Experimentelle Epilepsieforschung, Westfälische Wilhelms-Universität Münster, Hüfferstr. 68, 48149 Münster, Germany (T. B., H.-C. P.)

Abteilung für Klinische Neurobiologie, Universität Heidelberg, Im Neuenheimer Feld 364, 69120 Heidelberg, Germany (M. I. A., W. W.)

Institut für Physiologie, Otto-von-Guericke-Universität, Leipziger Str. 44, 39120 Magdeburg, Germany (T. M.)

Institut für Physiologie I, Westfälische Wilhelms-Universität Münster, Robert-Koch-Str. 27a, 48149 Münster, Germany (T. B., T. S., H.-C. P.)

Klinik für Neurologie, Julius-Maximilians-Universität Würzburg, Josef-Schneider Str.11, 97080 Würzburg, Germany (S. G. M., T. Sch., C. K., H. W.)

Institute of Medical Sciences, University of Aberdeen, Foresterhill, Aberdeen, AB25 2ZD, Scotland, UK (W. W.)

Molecular Pharmacology Fast Forward. Published on January 19, 2006 as DOI: 10.1124/mol.105.020594
This article has not been copyedited and formatted. The final version may differ from this version.

**Running title:** TASK-1 function in the thalamus

**Corresponding author:** Dr. Thomas Budde, Institut für Experimentelle Epilepsieforschung, Westfälische Wilhelms-Universität Münster, Hüfferstr. 68, D-48149 Münster, Germany

| | |
|---|---|
| **Number of text pages:** | 32 |
| **Number of tables:** | 0 |
| **Number of figures:** | 6 |
| **Number of references:** | 38 |
| **Number of words in the Abstract:** | 237 (250) |
| **Number of words in the Introduction:** | 743 (750) |
| **Number of words in the Discussion:** | 1481 (1500) |

**List of non-standard abbreviations:**

DLG - dorsal lateral geniculate nucleus

ECoG - electrocorticogram

K2P - two-pore domain potassium channels

TASK - Twik-related acid sensitive $K^+$ channel

TC - thalamocortical relay neuron

THIK - tandem pore domain halothane-inhibited $K^+$ channel

TREK - TWIK-related $K^+$ channel gene

## Abstract

A genetic knock out was used to determine the specific contribution of TWIK-related acid-sensitive $K^+$ (TASK-1) channels to the function of dorsal lateral geniculate nucleus (DLG) thalamocortical relay (TC) neurons. Disruption of TASK-1 function produced a ~19 % decrease in amplitude of the standing outward current ($I_{SO}$) and a 3 ± 1 mV depolarizing shift in resting membrane potential ($V_{rest}$) of DLG neurons. We estimated that current through TASK-1 homodimers or TASK1/TASK3 heterodimers contribute(s) about one third of the current sensitive to TASK channel modulators in DLG TC neurons. The effects of the TASK channel blocker bupivacaine (20 µM), of muscarine (50 µM), and of $H^+$ on $I_{SO}$ were reduced to about 60 %, 59 %, and shifted to more acidic pH values, respectively. The blocking effect of anandamide on $I_{SO}$ (30 µM; 23 ± 3 % current decrease in WT) was absent in TASK-1 knock out (TASK-$1^{-/-}$) mice (9 ± 6 % current increase). Comparable results were obtained with the more stable anandamide-derivative, methanandamide (20 µM; 20 ± 2 % decrease in WT; 4 ± 6 % increase in TASK-$1^{-/-}$). Current-clamp recordings revealed a muscarine-induced shift in TC neuron activity from burst to tonic firing in both mouse genotypes. Electroencephalographic and sleep/wake times were unchanged in TASK-$1^{-/-}$ mice. In conclusion our findings demonstrate a significant contribution of TASK-1 channels to $I_{SO}$ in DLG TC neurons, although the genetic knock out of TASK-1 did not produce severe deficits in the thalamocortical system.

## Introduction

K2P potassium channels contribute to the leak conductance that helps maintain negative resting membrane potentials (Brown, 2000; Lesage and Lazdunski, 2000; Patel and Honore, 2001). The fifteen mammalian K2P channel proteins are divided in six subfamilies based on sequence identities and functional features (Patel and Lazdunski, 2004). K2P subunits assemble as dimers (Plant et al., 2005) and some may be heterodimers. Whereas some channel subunits mediate time- and voltage-independent potassium leak currents, other subtypes, including TASK channels, increase their open probability with depolarization. Most K2P channels can be actively modulated; for example, many neurotransmitters/neuromodulators act via G-protein-coupled receptors to close TASK channels and so depolarize the cell, producing a change from burst to tonic firing in the case of DLG neurons (Meuth et al., 2003; Millar et al., 2000; Talley et al., 2000).

The current through TASK-1 and -3 subunits reveals outward-rectification of whole-cell currents under physiological $K^+$ concentrations and is inhibited by acidic pH; in recombinant systems and *in vivo,* channel subunits can assemble heteromerically if the cell type expresses both genes at suitable levels (Aller et al., 2005; Berg et al., 2004; Czirjak and Enyedi, 2002; Kang et al., 2004); alternatively, they can function as homomers if either TASK-1 or TASK-3 dominates the expression (Clarke et al., 2004; Czirjak and Enyedi, 2003). Due to (i) overlapping gene expression patterns, (ii) similarities of whole-cell currents through different channel subtypes, and (iii) the formation of heterodimeric channels resulting in intermediate properties, it is hard to specify the molecular origins of native leak currents. Thus knock out mice are valuable to assess the *in vivo* contributions and functional roles of specific K2P channel subtypes.

For example, previous work with TASK-1 knock out mice (TASK-$1^{-/-}$) dissected K2P channel diversity in adult cerebellar granule cells (Aller et al., 2005). Granule cells strongly express four K2P genes: TASK-1, TASK-3, the TREK-2c splice variant and THIK-2. In TASK-1 knockout mice, although the $I_{KSO}$ remained unchanged, and granule cells were not more depolarized, the standing outward $K^+$ current ($I_{KSO}$) became $Zn^{2+}$-sensitive, suggesting that normally most TASK channels in granule cells are TASK-1/TASK-3 heteromers, and that in the TASK-$1^{-/-}$ granule cells, this heteromer was replaced by homomeric TASK-3 channels. The failure to see a reduction in $I_{KSO}$ magnitude in the TASK-$1^{-/-}$ granule cells could be due to contributions from the remaining K2P genes.

By contrast, not all neuronal cell types express the high K2P channel diversity found in cerebellar granule cells. For example, the main K2P genes expressed in mouse thalamus are TASK-1, TASK-3 and TWIK-1. The TASK-3 gene dominates; however, there are variations in expression depending on the exact thalamic nucleus (see Figure 1). The DLG in the mouse thalamus contains moderate levels of TASK-3 and TASK-1 transcripts, together with some TWIK-1 and other K2P gene transcripts (Aller et al., 2005); indeed, in postnatal day 19 rat DLG cells in slices, both TASK-1 and TASK-3 channels (as assayed by pharmacology and *in situ* hybridization) significantly contribute to the unique features of the cells (Meuth et al., 2003), although under certain circumstances (removal of covalently attached SUMO protein), TWIK-1 has TASK-like channel properties (Rajan et al., 2005). Furthermore, in addition to the contribution from TASK channels, $I_{SO}$ in TC neurons is carried by additional channel types (persistent $Na^+$ channels, inward rectifying $K^+$ channels, non-inactivating voltage-dependent $K^+$ channels, pacemaker channels; S.G.M. & T.B., unpublished observations). But in any case, removing expression of a particular K2P family member from any given thalamic relay nucleus might have stronger impact on function than in cerebellar granule cells, simply because there are fewer other K2P channel types expressed in the thalamus which could compensate for the loss.

The likely function for K2P channels in thalamic relay cells is characterized by the closure of TASK-1/-3 channels mediated by modulatory transmitters such as acetylcholine acting via G-proteins thereby promoting membrane depolarization and a shift in activity mode from burst to tonic firing of action potentials (McCormick, 1992; Meuth et al., 2003; Steriade et al., 1997). To determine the specific contribution of the two TASK subunit variants to the physiology of DLG TC neurons and to analyze their influences on cell's response to cholinergic modulation we used TASK-1 deficient mice (TASK-$1^{-/-}$) (Aller et al., 2005). We addressed the following questions: (1) What are the pharmacological and functional consequences of a TASK-1 knock out in DLG cells and does it differ in its effects from cerebellar granule cells? (2) Is there a TASK-$1^{-/-}$ phenotype related to the thalamocortical system?

## Methods and Materials

### *The TASK-1 knockout mouse line*

The generation of TASK-1$^{-/-}$ mice has recently been described (Aller et al., 2005). For the study described here, and as in Aller et al 2005, TASK-1$^{-/-}$ mice were always produced by breeding heterozygote +/- animals; the -/- and +/+ littermates could then be used for direct comparisons. Mice were genotyped by Southern blotting (Aller et al., 2005).

### *Animals*

Mice were individually housed in standard cages without running wheels on a 12h / 12h light-dark cycle at an ambient temperature of 23 ± 1°C. Rodent laboratory chow and drinking water were provided *ad libidum*. All procedures involving the use of animals were approved by the local Animal Care Committee of the Universities of Heidelberg and Magdeburg in agreement with the German laws for animal protection.

### *In situ hybridization*

*In situ* hybridization, with $^{35}$S-labelled TASK-1 and TASK-3-specific oligonucleotide probes was performed as described (Aller et al., 2005). Brains were from wild-type P19 animals.

### *Preparation: thalamic slices*

Wild type (WT) and TASK-1 knock out mice (TASK-1$^{-/-}$) postnatal days 14-22 were deeply anaesthetized using halothane and decapitated as described earlier for rats (Meuth et al., 2003). In brief, thalamic slices were prepared as coronal sections on a vibratome (Series 1000

Classic, St. Louis, USA) in an ice-chilled solution containing (mM): Sucrose, 200; PIPES, 20; KCl, 2.5; $NaH_2PO_4$, 1.25; $MgSO_4$, 10; $CaCl_2$, 0.5; dextrose, 10; pH 7.35 adjusted with NaOH. Prior to the recording procedure, slices were kept submerged in artifical cerebrospinal fluid (ACSF, mM): NaCl, 125; KCl, 2.5; $NaH_2PO_4$, 1.25; $NaHCO_3$, 24; $MgSO_4$, 2; $CaCl_2$, 2; dextrose, 10; pH adjusted to 7.35 by bubbling with a mixture of 95% $O_2$ and 5% $CO_2$.

### *Patch-clamp recordings of DLG neurons*

DLG neurons were visualized in the slice preparation using a microscope equipped with infrared-differential interference contrast optics. Whole-cell recording pipettes were prepared from borosilicate glass (GT150T-10, Clark Electromedical Instruments, Pangbourne, UK) having typical resistances of 2-3 MΩ. Pipettes were filled with an intracellular solution containing (in mM): K-gluconate, 95; $K_3$-citrate, 20; NaCl, 10; HEPES, 10; $MgCl_2$, 1; $CaCl_2$, 0.5; BAPTA, 3; Mg-ATP, 3; Na-GTP, 0.5. In divalent-cation-free external solutions the osmolarity was kept constant at 305 mOsm / kg by adding mannitol. The internal solution was set to a pH of 7.25 with KOH and an osmolarity of 295 mOsm/kg. For current clamp recordings a pipette solution containing 5 mM EGTA and 0.5mM $CaCl_2$ was used. Slices were continuously superfused with a solution containing (in mM): NaCl, 120; KCl, 2.5; $NaH_2PO_4$, 1.25; HEPES, 30; $MgSO_4$, 2; $CaCl_2$, 2; dextrose, 10; and pH values were adjusted using HCl. Whole-cell patch-clamp recordings were measured with an EPC-10 amplifier (HEKA Elektronik, Lamprecht, Germany), digitized and acquired onto computer using Pulse software (HEKA Elektronik, Lamprecht, Germany).

All cells had a resting membrane potential more negative than -65mV, the access resistance was in the range of 5-15 MΩ and series resistance compensation of more than 40% was routinely used. A liquid junction potential of 8 ± 2 mV (n = 10) was measured and taken into account.

The pH-response curve of the standing outward current at -28 mV was drawn according to the equation $I_{SO} = I_{max} / \{1 + (EC_{50} / A)^n\}$, where $I_{SO}$ represents the current response, $I_{max}$ the maximal relative current amplitude, $EC_{50}$ the half-maximal effective pH value, A the pH value, and n the Hill coefficient.

### *Drugs*

The following drugs were used for electrophysiological recordings: bupivacaine and muscarine were obtained from Sigma (Deisenhofen, Germany), prepared as stock solutions in distilled water, and added to the perfusion medium. ZD7288 was delivered from Tocris (Köln, Germany) and prepared as above. Anandamide, methanandamide and arachidonic acid were obtained from Calbiochem (Schwalbach/Ts., Germany) and dissolved in ethanol. The solvent concentration in the final recording solution did not exceed 1%. Application of the solvent alone (1%) had no effect on the recorded current.

### *Surgery and electrode implantation*

Experiments were performed on male mice (aged between 8 weeks and 12 weeks, n = 5 for TASK-$1^{-/-}$- and wild-type littermates, respectively) and were approved by the Landesverwaltungsamt Halle (AZ 2-663Uni Magdeburg). Following anaesthesia with pentobarbital (50 mg/kg i.p., Sigma Chemical Co., St. Louis MO, USA) the mouse was positioned in a stereotaxic instrument (Kopf Instruments) with bregma and lambda in a horizontal plane. For bilateral epidural electrocorticogram (ECoG) recordings, silver electrodes were positioned over the central region (AP -1.0 mm, L 2 mm from bregma) of both hemispheres and fixed on the skull with dental acrylic cement (Paladur; Heraeus Kulzer GmbH, Wehrheim/Ts, Germany). Additionally, reference and ground electrodes were implanted over the nasal and cerebellar region, respectively. Xylocaine cream (2%, ASTRA, Germany) was applied to all pressure points and wound edges. Four days after surgery ECoG was recorded for 4 to 6 hours to get a wide spectrum of different behavioral states (i.e. wake, sleep) using a swivel commutator.

ECoG recordings were performed using the spike2-software package (Cambridge Electronic Design, Cambridge, U.K.). Recorded electrical activities were fed through a differential amplifier (EXT-20F or DPA 2F; npi electronic GmbH, Tamm, Germany) collected at a sampling rate of 1 kHz with a filter cutoff of 100 Hz, transformed by an A/D interface (CED 1401plus; Cambridge Electronic Design, Cambridge, U.K.) and stored on-line on a personal computer. Additionally, data were stored on a magnetic tape recorder via a neuro-corder (DR-890, NeuroData, Instr. Corp., Delaware Water Gap PA, USA) for off-line analysis.

### *Behavioural observations*

The activity of WT (n = 5; 27.58 ± 3g) and TASK-1$^{-/-}$ mice (n = 8; 28.39 ± 1.4g) was continuously recorded in their home cages by infrared detectors for 24h. These recordings were analyzed by two experienced observers blinded for the genetic background of the animals. Forms of behavior (sleep, resting, leaning, rearing, grooming, nutrition and moving) were calculated as percentage of 24h.

### *Statistics*

All results are presented as mean ± SEM and differences were considered statistically significant if $p < 0.05$. Substance effects were tested for statistical significance using a modified student´s t-test for small samples (Dixon and Massey, 1969).

## Results

### *Expression of the TASK-1 and TASK-3 genes in the mouse DLG*

We first examined the DLG by *in situ* hybridization and focused on the expression of the TASK-1 and -3 genes in our target thalamic nucleus. Mouse brains were selected from an age that matched the majority of electrophysiological recordings, postnatal day 19. Figure 1 shows coronal brain sections through the thalamus at the DLG level. We reported previously for the adult mouse brain (Aller et al., 2005), that the TASK-1 gene's highest expression is in cerebellar granule cells, motor neurons, raphe and locus ceruleus, whereas TASK-3 gene expression is at higher levels throughout the brain (e.g. CA1 pyramidal cells, dentate granule cells, neocortex, many hypothalamic nuclei). This is reflected in the coronal images shown in Figure 1 at the level of the thalamus for P19. Nevertheless, specific thalamic nuclei have quite different expression profiles of the TASK-1 and TASK-3 genes. For example, the ventral lateral geniculate nucleus (VLG) has more TASK-3 than TASK-1 gene expression, whereas the midline thalamic nuclei have more TASK-1 transcripts (Fig. 1A, 1C). More caudally (Figs. 1B, 1D), TASK-3 expression dominates in the thalamus and zona incerta (ZI, Fig. 1D). TASK-1 expression dominates in the reticular thalamus (Fig. 1A, Rt). Despite the overall predominance of TASK-3 gene expression in the fore- and midbrain, both TASK-1 and TASK-3 mRNAs can be detected in the DLG at about roughly equal amounts (Fig. 1 A, C, DLG).

### *pH sensitivity of leak potassium channels in WT and TASK-1$^{-/-}$ DLG neurons: consequences for the resting membrane potential*

TASK-1 and 3 channels contribute to the standing outward current ($I_{SO}$, cf. Fig. 3A) in several cell types, like cerebellar granule cells, motor neurons and DLG TC cells (Millar et al 2000; Bayliss et al., 2003; Brickley et al., 2001; Meuth et al., 2003). To assess the contribution of the TASK-1 subunit to the total TASK-1/-3 current in TC neurons of the DLG, we probed a number of TASK-1/3 channel features (pH-sensitivity, block by bupivacaine, modulation by ACh) in whole-cell patch-clamp experiments. Both TASK-1 and TASK-3 channels are inhibited by acidification, although over different pH ranges (pK values for channel activity, ~7.5 and ~6.7 for TASK-1 and TASK-3, respectively) (Duprat et al., 1997; Kim et al., 2000; Rajan et al., 2000). Tandem-linked heterodimeric TASK channel constructs displayed pH sensitivity (pK ~7.3) closer to that of TASK-1 than TASK-3 (Berg et al., 2004). In a first experimental step we compared the pH-dependency of $I_{SO}$ in wild type (WT) and TASK-1$^{-/-}$ mice. At a holding potential of -28 mV $I_{SO}$ averaged 368 ± 17 pA in WT mice (n = 38) and 299 ± 16 pA in TASK-1$^{-/-}$ mice (n = 37; data not shown; p = 0.005) under experimental control conditions (pH 7.25). Varying the external pH ($pH_O$) from 8.0 to 5.0 stepwise resulted in a reduction of $I_{SO}$ which was different in both genotypes. Whereas $I_{SO}$ averaged 438 ± 47 pA (n = 4) and 415 ± 32 pA (n = 3) at pH 7.5 in WT and TASK-1$^{-/-}$, respectively, current amplitudes were strongly reduced to 39 ± 22 pA (n = 4; WT) and 35 ± 29 pA (n = 3; TASK-1$^{-/-}$) at pH 5.0. From populations of cells (a total of 24 cells were tested for each genotype) recorded at different pH values the $EC_{50}$ value of $I_{SO}$ inhibition could be determined at 6.6 and 5.9 for WT and TASK-1 $^{-/-}$, respectively, according to the Hill equation (Fig. 2A).

Next we determined the resting membrane potential ($V_{rest}$) of DLG TC neurons. In accordance with the averaged $I_{SO}$ amplitudes and the knock out of a hyperpolarizing membrane current, $V_{rest}$ under control conditions ($pH_O$ = 7.25) was significantly ($p < 0.009$) more negative than in WT (-73 ± 1 mV, n = 19) compared to TASK-1$^{-/-}$ (-70 ± 1 mV, n = 10; Fig. 2B). This difference was sustained when the depolarizing pH-sensitive current through HCN channels, the $I_h$ current, was blocked by ZD7288 (BoSmith et al., 1993) (WT: -83 ± 1 mV, n = 11; TASK$^{-/-}$: -76 ± 2 mV, n = 8; Fig. 2B). Subsequent reduction of $pH_O$ to 5.0 resulted in strong depolarization of $V_{rest}$ to values which were not different between the knockout and wild type littermates (WT: -34 ± 4 mV, n = 3; TASK-$1^{-/-}$: -35 ± 3 mV, n = 4; Fig. 2B). In summary these data indicate reduced $I_{SO}$ amplitude and depolarized $V_{rest}$ in DLG cells lacking TASK-1 expression.

### *Actions of the local anesthetic bupivacaine on $I_{SO}$ in DLG neurons*

Next, the local anesthetic bupivacaine, known to block TASK-1 and -3 channels (Kindler et al., 1999; Leonoudakis et al., 1998; Meadows and Randall, 2001; Meuth et al., 2003) was tested. Bath application of 20 µM bupivacaine resulted in a marked reduction in $I_{SO}$ amplitude which was significantly (p = 0.027) stronger in WT (55 ± 8 %; n = 8) compared with TASK-$1^{-/-}$ (33 ± 4 %; n = 8; Fig. 3A, B, D). To determine the current-voltage (*I/V*) relationship of the bupivacaine-sensitive current the membrane potential was ramped from -28 mV to -138 mV over 800 ms (Fig. 3A, 3B, inset). The resulting current revealed a complex waveform indicative for outwardly and inwardly rectifying components (Fig. 3A, 3B). By subtracting currents in the presence of bupivacaine from control currents, and assigning the appropriate membrane potential to each time point, the *I-V* relationship of the bupivacaine-sensitive current was constructed (Fig. 3C). The bupivacaine-sensitive currents in DLG neurons revealed clear outward rectification and a reversal potential of -103 ± 5 (n = 8) and of -103 ± 3 (n = 8) for WT and TASK-$1^{-/-}$, respectively, i.e. close to the expected $K^+$ equilibrium potential ($E_K$) of -104 mV. In summary these data indicate a reduced bupivacaine-sensitive current component in DLG neurons lacking TASK-1 gene expression.

### *Muscarine inhibits $I_{SO}$ in WT and TASK-$1^{-/-}$ DLG cells: functional implications*

Next, we investigated the functional modulation of TASK-1 and -3 channels in DLG neurons by activation of muscarinic ACh receptors (mAChR). First, the action of muscarine (50 µM) was analyzed under voltage-clamp conditions. Following application of muscarine via the extracellular solution $I_{SO}$ amplitude was significantly ($p = 0.025$) reduced by 41 ± 2 % ($n = 4$) and 24 ± 4 % ($n = 8$) in WT and TASK-$1^{-/-}$, respectively (Fig. 4A, B, D). The curvature of the muscarine-sensitive *I-V* relationship was characterized by inward and outward rectification in both genotypes and reversed close to $E_K$ (WT: -105 ± 5 mV, $n = 4$; TASK-$1^{-/-}$: -107 ± 2 mV, $n = 8$; Fig. 4C). Second, the effect of mAChR activation was recorded under current-clamp conditions. In order to allow high-frequency burst firing, cells were held at a potential of -72 ± 1 mV ($n = 8$) via DC current injection.

Depolarizing current steps (100-150 pA) evoked a typical burst of 2-5 action potentials riding on top of a low-threshold calcium spike (Steriade et al., 1997) in both mouse genotypes (Fig. 4E, F; black traces). The intra-burst frequency was 123 ± 2 Hz ($n = 4$) and 126 ± 1 Hz ($n = 4$) for WT and TASK-$1^{-/-}$, respectively. Bath application of muscarine (50 µM) induced a depolarizing shift in membrane potential which was not different between littermates (WT: 23 ± 2 mV, $n = 6$; TASK-$1^{-/-}$: 21 ± 3 mV, $n = 6$). This depolarization was accompanied by a switch in firing mode from burst to tonic generation of action potentials (Fig. 4E, F, grey traces). The frequency of tonic firing as derived from the first two spikes was 27 ± 4 Hz ($n = 4$) and 32 ± 3 Hz ($n = 4$) for WT and TASK-$1^{-/-}$, respectively. All effects were fully reversible (data not shown). In summary these data show that despite a reduction of the muscarine-sensitive current component, the functional impact of mAChR activation is not significantly changed in the two mice genotypes.

### *The effects of cannabinoid ligands on $I_{SO}$ in DLG neurons and the specific involvement of TASK-1*

The cannabinoid agonists anandamide (arachidonylethanolamide, 30 µM) and R-(+)-WIN 55, 212-2 have been suggested as TASK-1-specific blockers, having no effect on TASK-3 channels (Maingret et al., 2001). In contrast other reports have claimed that on recombinant channels anandamide does not distinguish between TASK-1 and TASK-3 (Aller et al., 2005; Berg et al., 2004). In the present study anandamide induced a reduction in $I_{SO}$ amplitude at -28 mV by 23 ± 3 % (n = 5; Fig. 5B, black bar) in WT neurons. In TASK-1$^{-/-}$ DLG neurons the blocking effect of anandamide was abolished and drug application was accompanied by a 9 ± 6 % (n = 6; Fig. 5B, grey bar) increase in $I_{SO}$ amplitude. The *I-V* relationship of the anandamide-sensitive current in WT neurons was characterized by outward rectification and reversed at -103 ± 3 mV (n = 5; Fig. 5A, black trace). In contrast the anandamide-sensitive current in TASK-1$^{-/-}$ DLG TC cells was linear and see-sawed around zero (n = 6; Fig. 5A, black circles). To confirm this data we used an anandamide analogue (methanandamide; 10 µM) with higher metabolic stability. Whereas application of methanandamide onto WT neurons reduced $I_{SO}$ amplitude by 20 ± 2 % (n = 6; Fig. 5B, stripped black bar), the effect was absent on TASK-1$^{-/-}$ DLG cells (4 ± 6 % increase in $I_{SO}$ amplitude; n = 6; Fig. 5B, grey stripped bar). The *I-V* relationship of the methanandamide-sensitive current was characterized by outward rectification and a reversal potential at -105 ± 2 mV (n = 6; Fig. 5A, grey trace). In TASK-1$^{-/-}$ DLG cells the methanandamide-sensitive current was linear with near zero amplitude (n = 6; Fig. 5A, grey circles). Since anandamide can be rapidly transformed to arachidonic acid (AA), we next investigated the effect of this eicosanoid on $I_{SO}$ in DLG TC neurons. In both TASK-1$^{-/-}$ and WT DLG cells, AA induced a significant increase in $I_{SO}$ amplitude and was thus very different from the effect of the two anandamide derivatives (WT: 25 ± 6 % increase, n = 5; TASK-1$^{-/-}$: 32 ± 9 %, n = 7; data not shown).

Since TASK-3 channels are specifically blocked by divalent cations (Clarke et al., 2004; Derst et al., 2002), we omitted $Ca^{2+}$ and $Mg^{2+}$ from the external recording solution. In both

TASK-1$^{-/-}$ and WT DLG cells, $I_{SO}$ amplitudes significantly increased after establishing divalent cation-free conditions (19 ± 2 %, n = 8, for WT; 18 ± 1 %, n = 4, for TASK-1$^{-/-}$; Fig. 5D), with the curvature of the *I-V* relationship of the divalent cation-sensitive current pointing to the contribution of outwardly and inwardly rectifying components. The current reversal was close to $E_K$ (-104 ± 2 mV for WT, Fig. 5C, black trace; -102 ± 3 mV for TASK1$^{-/-}$ mice, Fig. 5C, grey trace). These data demonstrate the absence of TASK-1-specific effects and an unchanged response to a TASK-3-specific experimental maneuver in TASK-1$^{-/-}$ DLG cells.

### *Electroencephalographic (EEG) recordings*

To assess possible deficits of TASK-1$^{-/-}$ mice with respect to whole brain function we recorded electrocorticograms (ECoG) of freely-moving TASK-1$^{-/-}$ and WT littermates. TASK-1$^{-/-}$ as well as WT mice expressed very regular field potential patterns on the ECoG without any abnormalities like polyspike complexes or high-voltage-spike activities and showed similar patterns during expression of different behavioral states (e.g. wake, sleep; data not shown). During wake behavioral state both genotypes revealed predominant frequencies at theta frequency (5-12 Hz). During sleep the ECoG of TASK-1$^{-/-}$ and WT animals was characterized by higher amplitudes compared to the wake state and low frequency activity at about 2-4 Hz (data not shown).

### *Behavioral observations indicate a comparable sleep-wake-cycle of TASK-1$^{-/-}$ mice and controls*

Since the dorsal thalamus plays an important role in the mammalian sleep-wake-cycle, we next performed behavioral observations on WT and TASK-1$^{-/-}$ mice. Consistent with the EEG recordings the behavioral observations offered similar results for both mice genotypes. With respect to sleeping and waking behavior WT animals were active (addition of moving, rearing, leaning, grooming and nutrition) and inactive (sleeping, resting) for 44 ± 2% and 56 ± 2% of the day (n = 5, repeated measurements, Fig. 6A). The behavior of TASK-1$^{-/-}$ mice was indistinguishable with 43 ± 1% active and 57 ± 1% inactive behavior per 24 hours (n = 5, repeated measurements, Fig. 6A). Furthermore the analysis of specific behaviors like moving, rearing, leaning, grooming or nutrition showed no statistical significant differences between knock outs and wild type littermates (Fig. 6B). Similarly, further differentiation of inactive behavior (separation of resting behavior and sleep) displayed no significant differences between the two groups.

Molecular Pharmacology Fast Forward. Published on January 19, 2006 as DOI: 10.1124/mol.105.020594
This article has not been copyedited and formatted. The final version may differ from this version.

## Discussion

This study describes novel aspects of TASK-1 channel function in DLG TC neurons and can be summarized as follows: (1) $I_{SO}$ amplitude was reduced and the resting membrane potential was more depolarized in TASK-1$^{-/-}$ cells in comparison with WT; (2) $I_{SO}$ decreased in amplitude with increasing proton concentration. The pK value of current inhibition was shifted to lower pH values in TASK-1$^{-/-}$ neurons compared with WT; (3) The TASK-1/-3 channel blocker bupivacaine reduced the outwardly rectifying TASK current in TASK-1$^{-/-}$ more effectively than in WT; (4) Muscarine reduced $I_{SO}$ by inhibiting TASK-1/3 channels and inwardly rectifying channels. Although this effect was less pronounced in knock outs, neurons switched from burst to tonic firing in both TASK-1$^{-/-}$ and WT. (5) Anandamide, as well as the more stable methanadamide blocked an outward rectifying TASK current component in WT but were ineffective in TASK-1$^{-/-}$. On the other hand, removal of divalent cations from the extracellular medium, a maneuver to specifically unblock TASK-3 channels, was equally effective in the two genotypes. (6) Consistent with the mild electrophysiological effects of TASK-1 gene knock out in the dorsal thalamus, no noticeable differences between WT and TASK-1$^{-/-}$ mice were found in EEG recordings and in the overall sleep/waking behavior. We conclude: (i) that in DLG neurons TASK-1 makes a significant contribution to $I_{SO}$ and (ii) that anandamide blocks TASK-1 or TASK-1/-3 channels in DLG TC cells, but not on the presumably homomeric TASK-3 channels remaining in the TASK-1$^{-/-}$ DLG TC cells.

### *TASK channels in DLG TC neurons*

The TASK channel genes are differentially expressed in the rodent CNS (Talley et al., 2001). In rat DLG TC neurons, the current carried by TASK channels is characterized by outward rectification, reversal at $E_K$, inhibition by extracellular acidification, block by bupivacaine, and down-regulation by activation of mAChR (Meuth et al., 2003). From the data presented here, we estimate that current through TASK-1 homodimers or TASK-1/TASK-3 heterodimers (Czirjak and Enyedi, 2002) contribute(s) about one third of the current sensitive to TASK channel modulators in DLG TC neurons. This conclusion is based on the following evidence: (1) Compared to WT, the bupivacaine-sensitve current in TASK-$1^{-/-}$ DLG TC neurons is about 35 % smaller in amplitude; (2) The difference between bupivacaine-sensitve currents in WT and TASK-$1^{-/-}$ DLG cells at -28 mV is about 100 pA; (3) Similar to the effect of bupivacaine, the muscarine-sensitive component is about 28 % smaller in TASK-$1^{-/-}$ DLG cells. These findings further indicate that bupivacaine (Brown, 2000; Buckler et al., 2000; Leonoudakis et al., 1998) and mechanisms acting downstream of mAChR (Patel and Lazdunski, 2004) influence TASK-1 and TASK-3 channels similarly. Nevertheless, knock out of the TASK-1 gene significantly reduced $I_{SO}$, resulting in a depolarized resting membrane potential, thereby confirming the persistent activity of native TASK-1 channels and their contribution to the neuronal membrane potential (Duprat et al., 1997). However, in adult cerebellar granule cells, deletion of the TASK-1 protein leaves the magnitude of $I_{KSO}$ unaffected (Aller et al., 2005), wheras deletion of TASK-1 from DLG TC cells produces a decrease in leak conductance. One explanation is that granule cells express more K2P subunit genes at higher levels than DLG TC cells, allowing greater possibilities of compensation (Brickley et al., 2001). Similar considerations may apply to other brain regions since the TASK-$1^{-/-}$ phenotype shows few neurological deficits.

Both, TASK1 and TASK3 channels are inhibited by acidification, although over different pH ranges (pK ~7.5 and ~6.7 for TASK1 and TASK3, respectively) (Duprat et al., 1997; Kim et al., 2000; Rajan et al., 2000). Tandem-linked heterodimeric TASK channel constructs displayed pH sensitivity (pK ~7.3) closer to that of TASK1 than TASK3 (Berg et al., 2004). Consistent with these findings $I_{SO}$ amplitude in TC cells of WT (TASK3 + TASK1; $EC_{50}$ = 6.6) revealed an $EC_{50}$ value that was shifted to a more alkaline pH value in comparison to $TASK1^{-/-}$ (TASK3 only; $EC_{50}$ = 5.9). Deviation of absolute pK values from those published for heterologously expressed TASK channels and the 90 % reduction of $I_{SO}$ at pH 5.0 probably result from the fact that the steady-state current in TC neurons is carried by a number of different ion channels (persistent $Na^+$ channels, inward rectifier $K^+$ channels, non-inactivating voltage-dependent $K^+$ channels, TASK channels, pacemaker channels; S.G.M. & T.B., unpublished observations) with unknown or undefined pH-sensitivity. Changes of the extracellular pH can influence a variety of different conductances and receptors (Kaila and Ransom, 1998), so that additional contributors to the pH effects can be expected.

### *Endogenous cannabinoids and their actions on TASK channels of DLG cells*

Human recombinant TASK-1 but not TASK-3 channels are blocked by anandamide (Maingret et al., 2001). However the situation seems to be more complicated when taking rodent TASK channels into account, since two other groups claim that anandamide blocks both recombinant (rodent) TASK-1 and TASK-3 channels fairly equally at concentrations > 1 µM (Aller et al., 2005; Berg et al., 2004). Surprisingly, we found that TASK-1 channels convey the anandamide-sensitivity of $I_{SO}$ in DLG TC neurons thereby confirming that the endogenous cannabinoid ligand anandamide compounds selectively block TASK-1 channels (Maingret et al., 2001). This conclusion is confirmed indirectly by the effect of specifically activating TASK-3 channels by removing extracellular divalent cations, which produced indistinguishable effects in the two mouse genotypes. Anandamide may be rapidly eliminated by enzymatic hydrolysis leading to the production of AA. The finding that AA induced an increase in $I_{SO}$ rather than a reduction further confirms the specific action of anandamide. Although we have no intuitive explanation for this selectivity of anandamide for TASK-1 in native membranes, the following findings should be taken into account: (1) At higher concentrations (10 µM) recombinant rodent TASK-1 channels are more sensitive to anandamide than rodent TASK-3 channels (Berg et al., 2004). (2) The anandamide-sensitive

Molecular Pharmacology Fast Forward. Published on January 19, 2006 as DOI: 10.1124/mol.105.020594
This article has not been copyedited and formatted. The final version may differ from this version.

current components in rat and mouse DLG TC neurons are similar: they outwardly rectify, reverse at $E_K$, and constitute 22 ± 2 % (n = 4) and 23 ± 3 % (n = 5) of $I_{SO}$, respectively. These findings may point to subtle cell type-specific influences. (3) TASK channels are regulated by adapter proteins and phosphatidylinositol-4,5-bisphosphate ($PIP_2$) (Chemin et al., 2003; Czirjak et al., 2001; Lopes et al., 2005; Rajan et al., 2002), thereby indicating complex interplays between multiple factors. (4) TASK-$1^{-/-}$ mice have changed responses to the cannabinoid ligand WIN55212-2 (Linden et al., 2004); the analgesic, sedative and hypothermic effects of WIN55212-2 are reduced in TASK-$1^{-/-}$ mice, implicating channels containing TASK-1 in supraspinal pain pathways, for example in the thalamus. This behavioral result confirms that endogenous cannabinoid ligands certainly have the potential to influence cell excitability by acting close to TASK-1 and/or TASK-3 channels *in vivo*.

### *TASK-1 function in the thalamocortical system*

The resting membrane potential of thalamic relay neurons is in the range of -70 mV and has been attributed to currents through leak channels ($I_{K\text{-leak}}$, $I_{Na\text{-leak}}$), pacemaker channels ($I_h$), inwardly rectifying $K^+$ currents ($I_{KIR}$), and voltage-dependent channels active below threshold ($I_A$, $I_T$) (Williams et al., 1997; Zhan et al., 1999). TASK-1 contributes ~3 mV hyperpolarization to $V_{rest}$ and partially counterbalances the depolarizing influence of $I_h$. Strong extracellular acidification completely inhibited current through TASK-1/-3 channels and resulted in a marked depolarization of $V_{rest}$ indicating some tens of mV hyperpolarizing influence of TASK channels. The value of the prevailing membrane potential in TC neurons is outstandingly important for thalamic function since these cells display burst activity and tonic firing at hyperpolarized and depolarized values of the membrane potential, respectively (Steriade et al., 1997). The burst mode of activity is characterized by two to six action potentials on the ridge of a low threshold calcium spike and occurs during natural sleep and absence epilepsy. Generation of single action potentials can be observed during wakefulness (Steriade et al., 1997). The shift between the two activity modes is mediated by transmitters of the ascending brain stem system (e.g., ACh) acting on $I_{K\text{-leak}}$ (McCormick, 1992). Recently it has been shown that TASK-1 and TASK-3 channels constitute the mAChR-sensitive leak current in TC neurons (Meuth et al., 2003). However, removal of TASK-1 is not sufficient to disrupt the mAChR-dependent switch from burst to tonic firing in DLG TC neurons *in situ*. Although the tonic firing frequency of TASK-1$^{-/-}$ TC neurons tends towards higher frequencies during ACh application (27 Hz and 32 Hz for WT and TASK-1$^{-/-}$, respectively), a comparison with cells from standard C57/BL6 wild-type mice revealed no significant differences (32 ± 2 Hz, n = 7, under identical recording conditions) thereby indicating similar tonic firing properties in different mouse genotypes. In accordance with this finding no behavioral deficits related to the function of the thalamocortical system, e.g. overall EEG pattern and sleeping/waking behavior could be observed for TASK-1$^{-/-}$ mice. It cannot be excluded, however, that sleep deprivation or some other induced stress would reveal functional differences between WT and TASK-1$^{-/-}$. We anticipate that TASK-3 and TASK-1/TASK-3 double or perhaps TASK-1/TASK-3/TWIK-1 triple knockouts will be needed to assess the full impact of K2P channel activity on thalamic function.

## Acknowledgments

Thanks are due to Mrs. I. Preugschat-Gumprecht (Heidelberg), Mrs. R. Ziegler (Magdeburg) and Mrs. A. Jahn (Magdeburg) for excellent technical assistance. W. W. thanks Prof. Dr. H. Monyer for generous support.

## References

Aller MI, Veale EL, Linden AM, Sandu C, Schwaninger M, Evans LJ, Korpi ER, Mathie A, Wisden W and Brickley SG (2005) Modifying the subunit composition of TASK channels alters the modulation of a leak conductance in cerebellar neurons. *J Neurosci* **25**:11455-11467.

Bayliss DA, Sirois JE and Talley EM (2003) The TASK family: two-pore domain background K+ channels. *Mol Interv* **3**(4):205-219.

Berg AP, Talley EM, Manger JP and Bayliss DA (2004) Motoneurons express heteromeric TWIK-related acid-sensitive $K^+$ (TASK) channels containing TASK-1 (KCNK3) and TASK-3 (KCNK9) subunits. *J Neurosci* **24**(30):6693-6702.

BoSmith RE, Briggs I and Sturgess NC (1993) Inhibitory actions of ZENECA ZD7288 on whole-cell hyperpolarization activated inward current (If) in guinea-pig dissociated sinoatrial node cells. *Br J Pharmacol* **110**(1):343-349.

Brickley SG, Revilla V, Cull-Candy SG, Wisden W and Farrant M (2001) Adaptive regulation of neuronal excitability by a voltage-independent potassium conductance. *Nature* **409**(6816):88-92.

Brown DA (2000) Neurobiology: the acid test for resting potassium channels. *Curr Biol* **10**(12):R456-459.

Buckler KJ, Williams BA and Honore E (2000) An oxygen-, acid- and anaesthetic-sensitive TASK-like background potassium channel in rat arterial chemoreceptor cells. *J Physiol* **525 Pt 1**:135-142.

Chemin J, Girard C, Duprat F, Lesage F, Romey G and Lazdunski M (2003) Mechanisms underlying excitatory effects of group I metabotropic glutamate receptors via inhibition of 2P domain $K^+$ channels. *Embo J* **22**(20):5403-5411.

Clarke CE, Veale EL, Green PJ, Meadows HJ and Mathie A (2004) Selective block of the human 2-P domain potassium channel, TASK-3, and the native leak potassium current, IKSO, by zinc. *J Physiol* **560**(Pt 1):51-62.

Czirjak G and Enyedi P (2002) Formation of functional heterodimers between the TASK-1 and TASK-3 two-pore domain potassium channel subunits. *J Biol Chem* **277**(7):5426-5432.

Czirjak G and Enyedi P (2003) Ruthenium red inhibits TASK-3 potassium channel by interconnecting glutamate 70 of the two subunits. *Mol Pharmacol* **63**(3):646-652.

Czirjak G, Petheo GL, Spat A and Enyedi P (2001) Inhibition of TASK-1 potassium channel by phospholipase C. *Am J Physiol Cell Physiol* **281**(2):C700-708.

Derst C, Liu GX, Musset B, Rajan S, Preisig-Müller R and Daut J (2002) Molecular analysis of divalent cation sensitivity of TASK channels. *Pflügers Arch* **443 (S2)**:P44-10.

Dixon WJ and Massey FJ (1969) *Introduction to statistical analysis*. McGraw Hill, New York.

Duprat F, Lesage F, Fink M, Reyes R, Heurteaux C and Lazdunski M (1997) TASK, a human background $K^+$ channel to sense external pH variations near physiological pH. *Embo J* **16**(17):5464-5471.

Kaila K and Ransom BR (1998) *pH and Brain Function*. Wiley-Liss, New York.

Kang D, Han J, Talley EM, Bayliss DA and Kim D (2004) Functional expression of TASK-1/TASK-3 heteromers in cerebellar granule cells. *J Physiol* **554**(Pt 1):64-77.

Kim Y, Bang H and Kim D (2000) TASK-3, a new member of the tandem pore K(+) channel family. *J Biol Chem* **275**(13):9340-9347.

Kindler CH, Yost CS and Gray AT (1999) Local anesthetic inhibition of baseline potassium channels with two pore domains in tandem. *Anesthesiology* **90**(4):1092-1102.

Leonoudakis D, Gray AT, Winegar BD, Kindler CH, Harada M, Taylor DM, Chavez RA, Forsayeth JR and Yost CS (1998) An open rectifier potassium channel with two pore domains in tandem cloned from rat cerebellum. *J Neurosci* **18**(3):868-877.

Linden AM, Aller MI, Vekovischeva O, Leppa E, Rosenberg PH, Wisden W and Korpi ER (2004) SENSITIVITY OF $K^+$ CHANNEL TASK-1 DEFICIENT MICE TO ANESTHETICS ISOFLURANE AND PROPOFOL. *SfN, Abstract Viewer/Itinerary Planner Online*.

Lopes CM, Rohacs T, Czirjak G, Balla T, Enyedi P and Logothetis DE (2005) PIP2 hydrolysis underlies agonist-induced inhibition and regulates voltage gating of two-pore domain K+ channels. *J Physiol* **564**(Pt 1):117-129.

Maingret F, Patel AJ, Lazdunski M and Honore E (2001) The endocannabinoid anandamide is a direct and selective blocker of the background K(+) channel TASK-1. *Embo J* **20**(1-2):47-54.

McCormick DA (1992) Neurotransmitter actions in the thalamus and cerebral cortex and their role in neuromodulation of thalamocortical activity. *Prog Neurobiol* **39**:337-388.

Meadows HJ and Randall AD (2001) Functional characterisation of human TASK-3, an acid-sensitive two-pore domain potassium channel. *Neuropharmacology* **40**(4):551-559.

Meuth SG, Budde T, Kanyshkova T, Broicher T, Munsch T and Pape H-C (2003) Contribution of TWIK-related acid-sensitive $K^+$ channel 1 (TASK1) and TASK3 channels to the control of activity modes in thalamocortical neurons. *J Neurosci* **23**(16):6460-6469.

Millar JA, Barratt L, Southan AP, Page KM, Fyffe RE, Robertson B and Mathie A (2000) A functional role for the two-pore domain potassium channel TASK-1 in cerebellar granule neurons. *Proc Natl Acad Sci U S A* **97**(7):3614-3618.

Oliver D, Lien CC, Soom M, Baukrowitz T, Jonas P and Fakler B (2004) Functional conversion between A-type and delayed rectifier K+ channels by membrane lipids. *Science* **304**(5668):265-270.

Patel AJ and Lazdunski M (2004) The 2P-domain K+ channels: role in apoptosis and tumorigenesis. *Pflugers Arch* **448**(3):261-273.

Plant LD, Rajan S and Goldstein SA (2005) K2P channels and their protein partners. *Curr Opin Neurobiol* **15**(3):326-333.

Rajan S, Plant LD, Rabin ML, Butler MH and Goldstein SA (2005) Sumoylation silences the plasma membrane leak K+ channel K2P1. *Cell* **121**(1):37-47.

Rajan S, Preisig-Muller R, Wischmeyer E, Nehring R, Hanley PJ, Renigunta V, Musset B, Schlichthorl G, Derst C, Karschin A and Daut J (2002) Interaction with 14-3-3 proteins promotes functional expression of the potassium channels TASK-1 and TASK-3. *J Physiol* **545**(Pt 1):13-26.

Rajan S, Wischmeyer E, Xin Liu G, Preisig-Muller R, Daut J, Karschin A and Derst C (2000) TASK-3, a novel tandem pore domain acid-sensitive $K^+$ channel. An extracellular histidine as pH sensor. *J Biol Chem* **275**(22):16650-16657.

Steriade M, Jones EG and McCormick DA (1997) *Thalamus*. Elsevier, Amsterdam.

Talley EM, Lei Q, Sirois JE and Bayliss DA (2000) TASK-1, a two-pore domain $K^+$ channel, is modulated by multiple neurotransmitters in motoneurons. *Neuron* **25**(2):399-410.

Talley EM, Solorzano G, Lei Q, Kim D and Bayliss DA (2001) CNS distribution of members of the two-pore-domain (KCNK) potassium channel family. *J Neurosci* **21**(19):7491-7505.

Williams SR, Toth TI, Turner JP, Hughes SW and Crunelli V (1997) The 'window' component of the low threshold $Ca^{2+}$ current produces input signal amplification and bistability in cat and rat thalamocortical neurones. *J Physiol (Lond)* **505**(Pt 3):689-705.

Zhan XJ, Cox CL, Rinzel J and Sherman SM (1999) Current clamp and modeling studies of low-threshold calcium spikes in cells of the cat's lateral geniculate nucleus. *J Neurophysiol* **81**(5):2360-2373.

**Footnotes**

Supported by DFG (BU 1019/5-2 to T. B., WI 1951/1-2 to W. W., Leibniz-program to H.-C. P.), the Volkswagen Stiftung I/78 554 (W. W.) and Fonds der Chemischen Industrie (W. W.).

## Figure legends

**Fig. 1: *In situ* hybridization showing TASK-1 (A, B) and TASK-3 (C, D) gene expression in the mouse (wild type) thalamus from P19, an age matching the electrophysiological recordings.** CA1, hippocampal CA1 region; Cx, neocortex; DG, dentate granule cells; DLG, dorsal lateral geniculate nucleus; Rt, reticular thalamus; VLG, ventral lateral geniculate nucleus; ZI, zona incerta. X-ray film autoradiographs, exposure time 4 weeks. Scale bar, 1 mm.

**Fig. 2: pH sensitivity of the standing outward current in WT and TASK-1$^{-/-}$ DLG neurons.** (**A**) The dependence of $I_{SO}$ at -28 mV on extracellular acidification (mean ± SE) for groups of 3-5 relay neurons in a range from pH 5.0 to 8.0 is shown. The curve was drawn according to the Hill equation through the data points for WT (black line) and TASK-1$^{-/-}$ (grey line), respectively. The $EC_{50}$, $I_{max}$, and Hill values were: WT, 6.6, 106.4, 0.53; TASK-1$^{-/-}$, 5.9, 101.4, 0.55. (**B**) Mean value of the resting membrane potential under different recording conditions (squares: control conditions; circles: presence of ZD7288; triangles: presence of ZD7288 at pH 5.0; WT closed symbols; KO = TASK-1$^{-/-}$, open symbols).

**Fig. 3: Effect of bupivacaine on TASK current in WT and TASK-1$^{-/-}$ DLG neurons.** (**A**, **B**) Currents evoked by ramping the membrane potential from -28 mV to -138 mV over 800 ms (see inset) under control conditions (black trace) and during application of bupivacaine (grey trace) in WT (**A**) and TASK-1$^{-/-}$ mice (**B**). (**C**) Mean *I-V* relationship of current components sensitive to bupivacaine obtained by graphical subtraction of currents during drug action from control currents (i.e., control – bupivacaine). Both components show a clear outward rectification and a reversal at the expected $E_K$. (**D**) Mean bar graph representation of $I_{SO}$ reduction at – 28 mV by bupivacaine in WT (black bar) and TASK-1$^{-/-}$ (grey bar).

Molecular Pharmacology Fast Forward. Published on January 19, 2006 as DOI: 10.1124/mol.105.020594

**Fig. 4: Muscarine effect on $I_{SO}$ in WT and TASK-1$^{-/-}$ DLG neurons.** (**A**, **B**) Membrane responses to ramp protocols (from -30 mV to -120mV over 800 ms; see inset) under control conditions (black traces) and during bath application of muscarine (grey traces) in WT (**A**) and TASK-1$^{-/-}$ DLG cells (**B**). (**C**) The mean *I-V* relationship of the muscarine-sensitive current was calculated by graphical subtraction of currents during drug action from those under control conditions (i.e, control - muscarine). (**D**) Mean bar graph representation of $I_{SO}$ reduction at -28 mV by muscarine in WT (black bar) and TASK-1$^{-/-}$ (grey bar). (**E**, **F**) Functional consequences of muscarine administration were tested under whole-cell current-clamp conditions in WT (**E**) and TASK-1$^{-/-}$ (**F**). DLG TC neurons of both mouse genotypes were held at a potential of 72 ± 1 mV (n = 8) by DC current injection. This holding current was not changed during the course of the experiment. Cells were challenged using 100 - 200 pA depolarizing current pulses (800 ms duration). Under control conditions depolarizing current pulses starting from hyperpolarized membrane potentials evoked typical burst firing (black traces). Addition of muscarine led to a marked depolarization of the membrane potential with a consecutive shift of the activity mode from burst to tonic firing (gray traces).

**Fig. 5: Specific pharmacological strategies of blocking TASK-1 and TASK-3 channels in DLG TC neurons.** (**A**) *I-V* relationship of anandamide- (black label) and methanandamide-sensitive (grey label) currents in WT (straight lines) and TASK-1$^{-/-}$ (circles). (**B**) Mean bar graph representation of $I_{SO}$ changes induced by anandamide (closed bars) and methanandamide (stripped bars) in WT (black label) and TASK-1$^{-/-}$ (grey label). (**C**) *I-V* relationship of divalent cation-sensitive currents in WT (black line) and TASK-1$^{-/-}$ (grey line). (**D**) Mean bar graph representation of $I_{SO}$ induced by removal of divalent cations from the extracellular solution at -28 mV in WT (black bar) and TASK-1$^{-/-}$ (grey bar).

**Fig. 6: Behavioral analysis of WT and TASK-1$^{-/-}$.** (**A**) Mean bar graph representation of active (black bars) and inactive (grey bars) periods in WT and TASK-1$^{-/-}$ (as indicated) in % of 24 h. (**B**) Pie diagram representation of distinct active (moving, rearing, leaning, grooming and nutrition) and inactive (resting, sleep) behavior components.

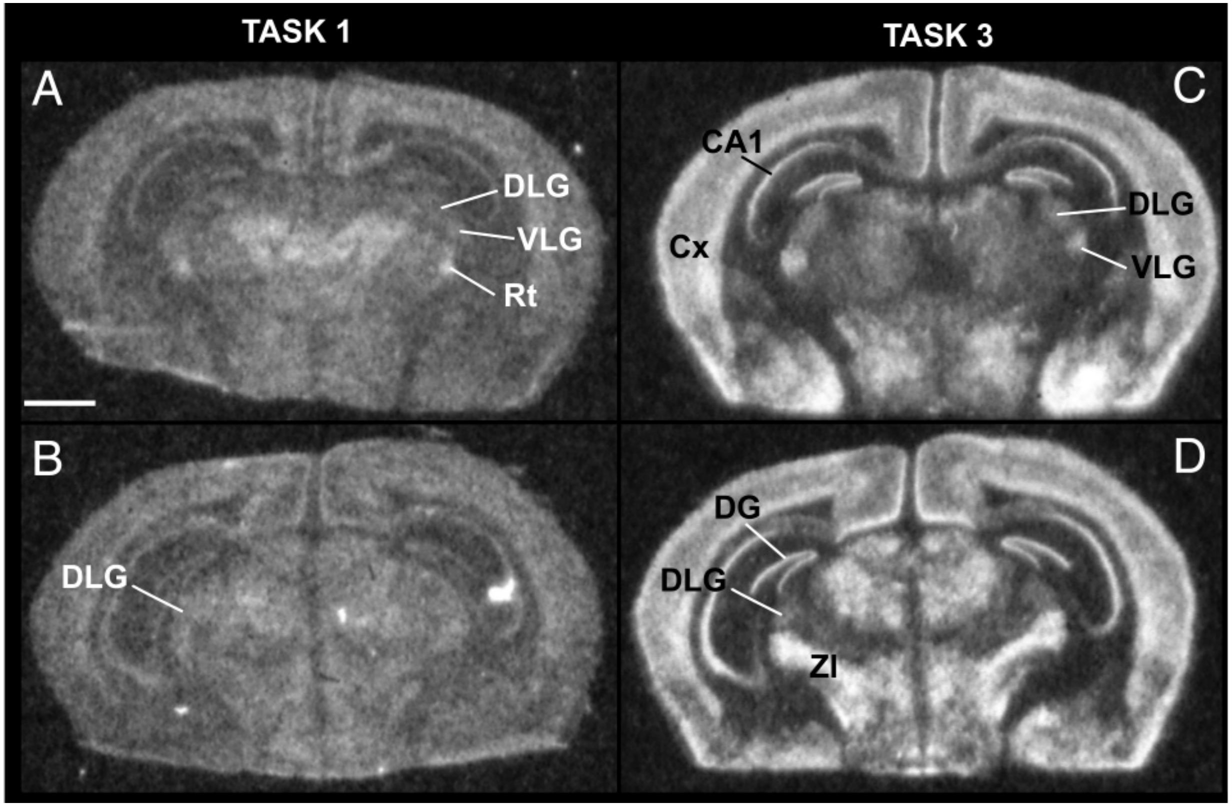
TASK 1
TASK 3
A
DLG
VLG
Rt
C
CA1
Cx
DLG
VLG
B
DLG
D
DG
DLG
ZI

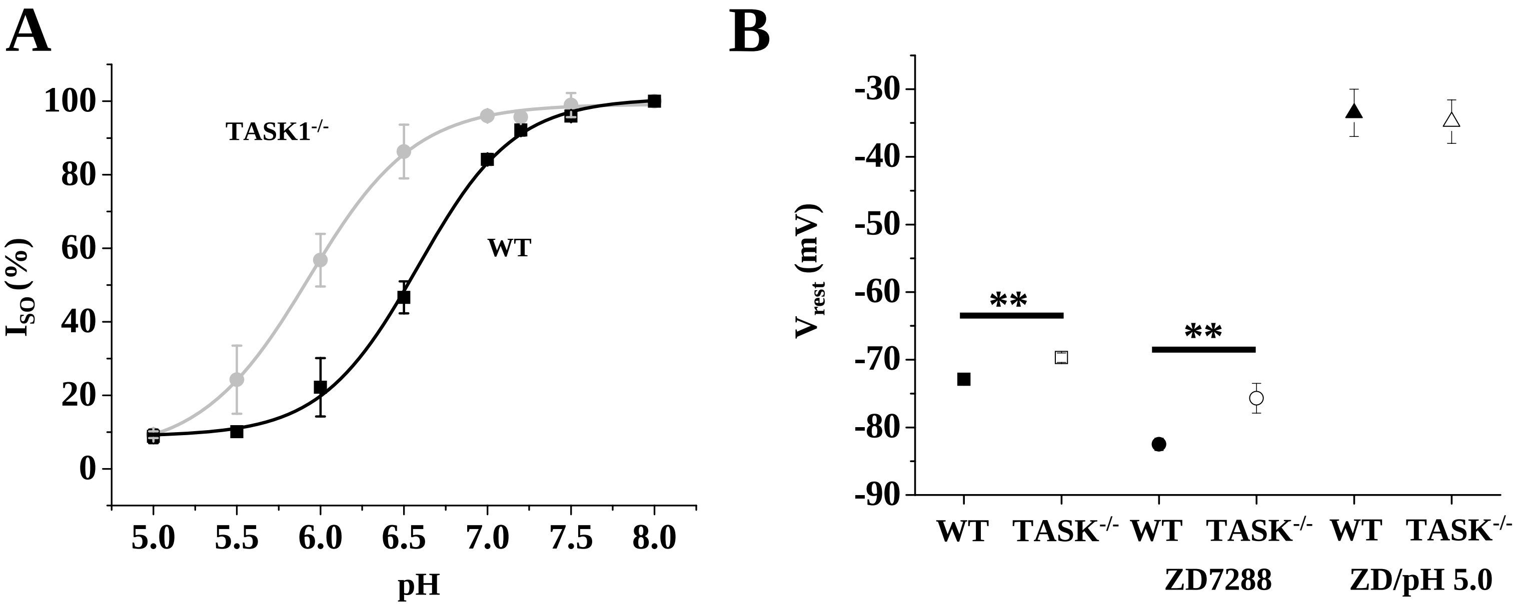
A
I_SO (%)
0
20
40
60
80
100
TASK1-/-
WT
5.0
5.5
6.0
6.5
7.0
7.5
8.0
pH
B
V_rest (mV)
-30
-40
-50
-60
-70
-80
-90
**
**
WT
TASK-/-
WT
TASK-/-
WT
TASK-/-
ZD7288
ZD/pH 5.0

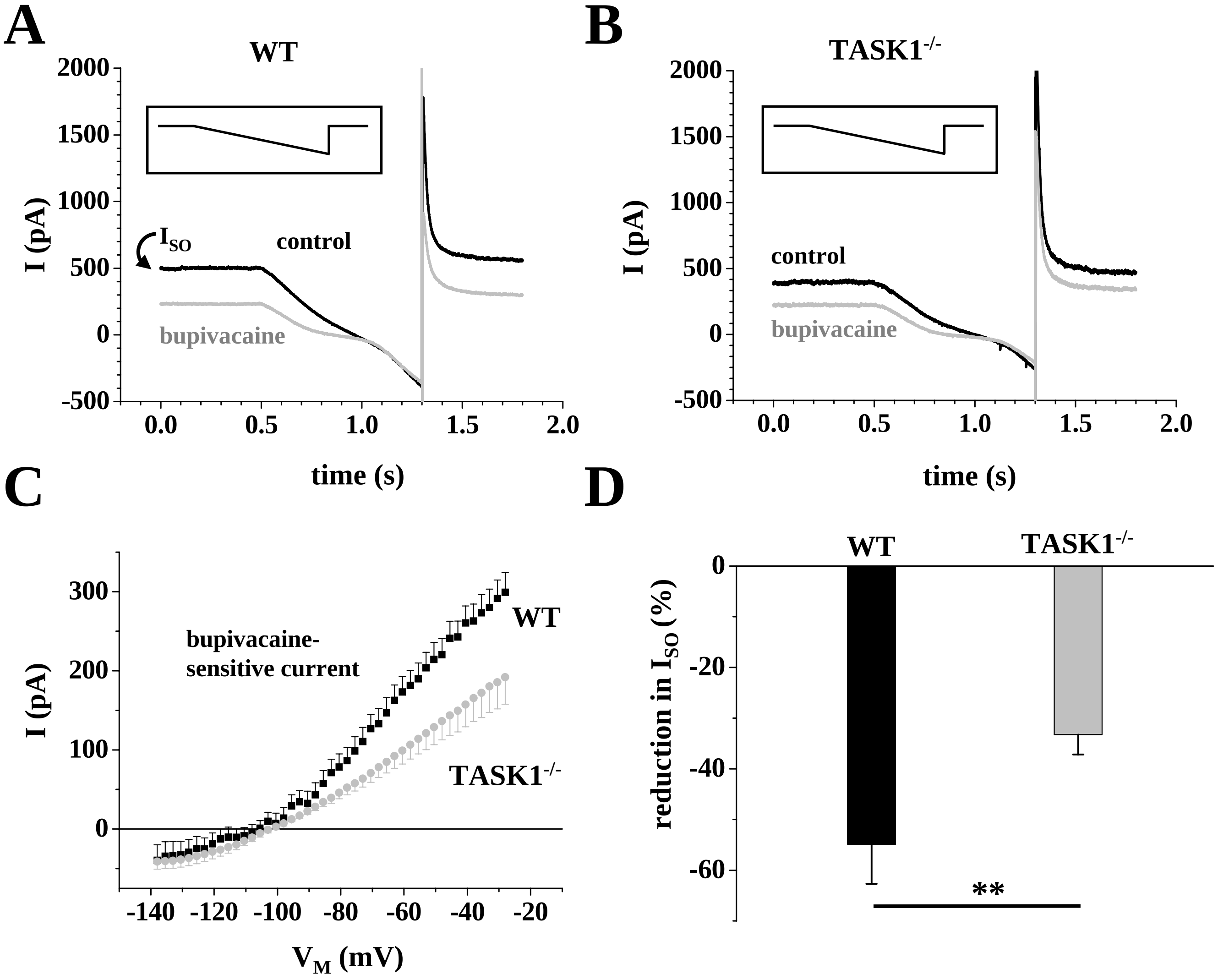
A
WT
B
TASK1$^{-/-}$
2000
1500
1000
500
0
-500
I (pA)
$I_{SO}$
control
bupivacaine
0.0
0.5
1.0
1.5
2.0
time (s)
C
D
300
200
100
0
bupivacaine-
sensitive current
WT
TASK1$^{-/-}$
-140
-120
-100
-80
-60
-40
-20
$V_M$ (mV)
reduction in $I_{SO}$ (%)
0
-20
-40
-60
**

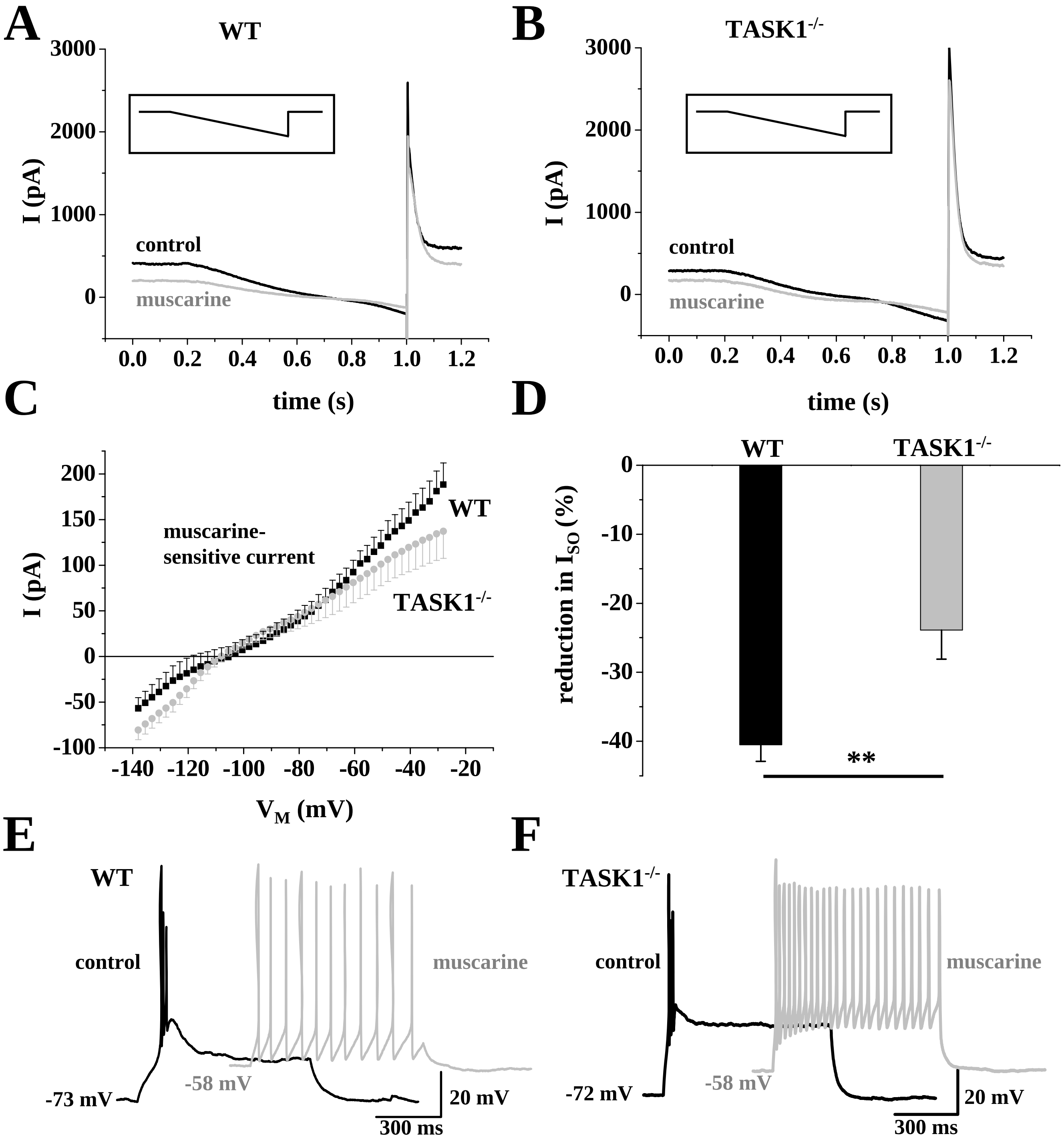
A
WT
3000
2000
1000
0
I (pA)
control
muscarine
0.0
0.2
0.4
0.6
0.8
1.0
1.2
time (s)
B
TASK1-/-
3000
2000
1000
0
I (pA)
control
muscarine
0.0
0.2
0.4
0.6
0.8
1.0
1.2
time (s)
C
200
150
100
50
0
-50
-100
I (pA)
muscarine-
sensitive current
WT
TASK1-/-
-140
-120
-100
-80
-60
-40
-20
V_M (mV)
D
WT
TASK1-/-
0
-10
-20
-30
-40
reduction in I_SO (%)
**
E
WT
control
muscarine
-73 mV
-58 mV
20 mV
300 ms
F
TASK1-/-
control
muscarine
-72 mV
-58 mV
20 mV
300 ms

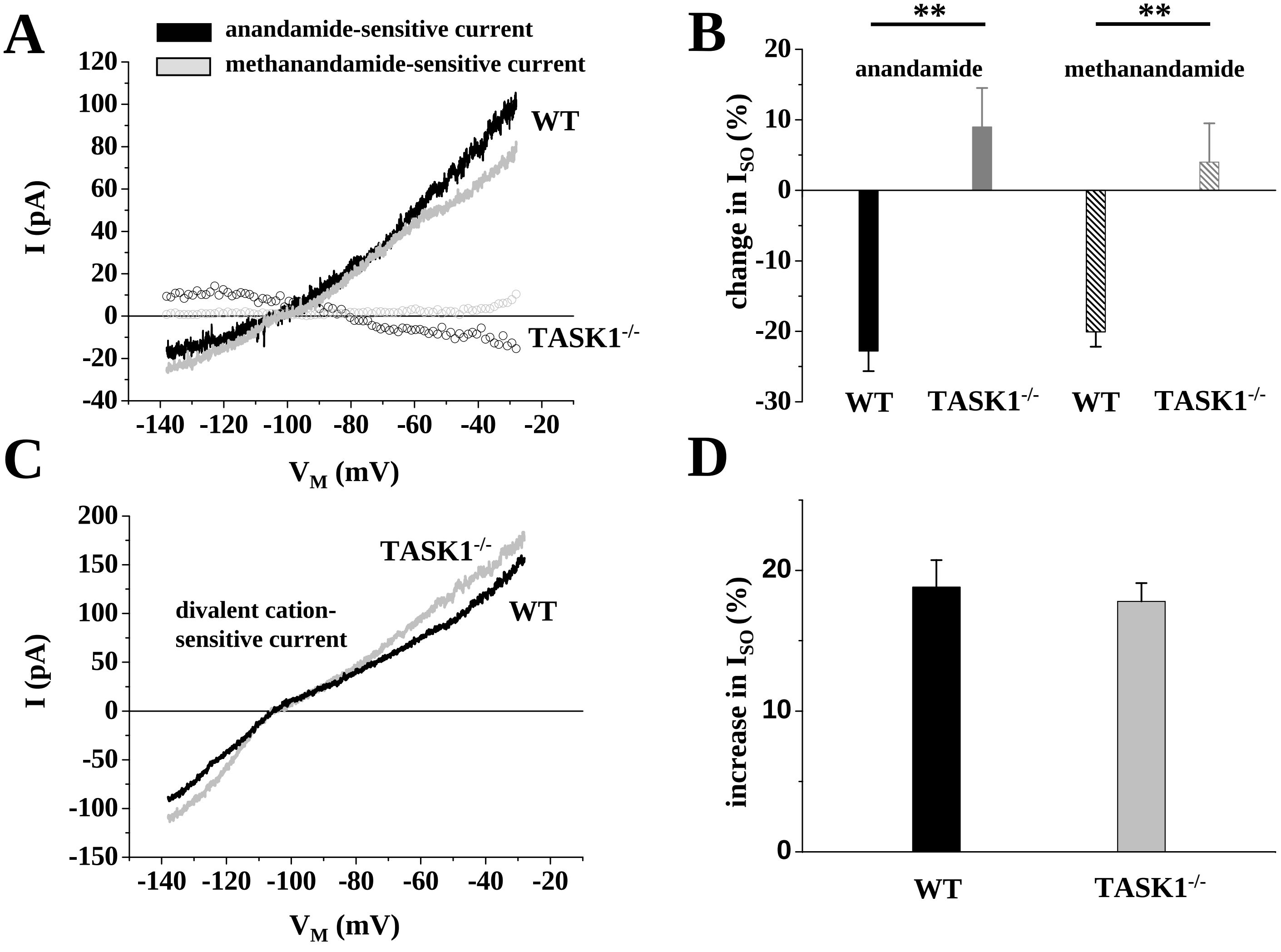
A
anandamide-sensitive current
methanandamide-sensitive current
120
100
80
60
40
20
0
-20
-40
I (pA)
WT
TASK1-/-
-140
-120
-100
-80
-60
-40
-20
V_M (mV)
B
**
**
anandamide
methanandamide
20
10
0
-10
-20
-30
change in I_SO (%)
WT
TASK1-/-
WT
TASK1-/-
C
200
150
100
50
0
-50
-100
-150
I (pA)
divalent cation-
sensitive current
TASK1-/-
WT
-140
-120
-100
-80
-60
-40
-20
V_M (mV)
D
20
10
0
increase in I_SO (%)
WT
TASK1-/-

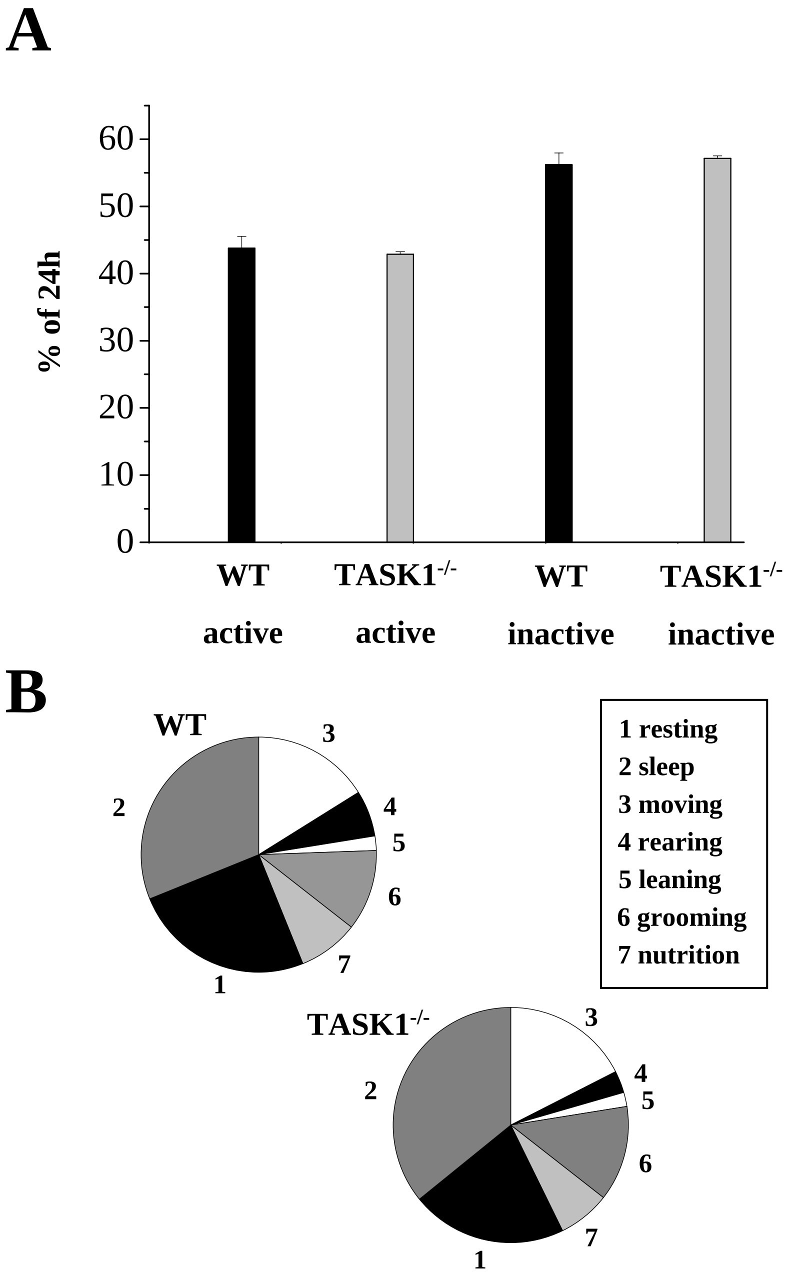
A
% of 24h
60
50
40
30
20
10
0
WT active
TASK1-/- active
WT inactive
TASK1-/- inactive
B
WT
TASK1-/-
1
2
3
4
5
6
7
1 resting
2 sleep
3 moving
4 rearing
5 leaning
6 grooming
7 nutrition